

## Field-Induced Self-Assembly of Suspended Colloidal Membranes

N. Osterman,<sup>1</sup> I. Poberaj,<sup>1,2</sup> J. Dobnikar,<sup>2,3</sup> D. Frenkel,<sup>3</sup> P. Zihler,<sup>1,2</sup> and D. Babić<sup>1</sup>

<sup>1</sup>Faculty of Mathematics and Physics, University of Ljubljana, Jadranska 19, SI-1000 Ljubljana, Slovenia

<sup>2</sup>Jožef Stefan Institute, Jamova 39, SI-1000 Ljubljana, Slovenia

<sup>3</sup>Department of Chemistry, University of Cambridge, Lensfield Road CB2 1EW, Cambridge, United Kingdom

(Received 2 September 2009; published 24 November 2009)

We report experiments that probe the self-assembly of micrometer-size colloids into one-particle-thick, robust, and self-healing membranes. In a magic-angle precessing magnetic field, superparamagnetic spheres experience isotropic pair attraction similar to the van der Waals force between atoms. But the many-body polarization interactions among them steer an ordered aggregation pathway consisting of growth of short chains, cross-linking and network formation, network coarsening, and consolidation of membrane patches. This generic aggregation scenario can be induced in any particles of large enough susceptibility.

DOI: 10.1103/PhysRevLett.103.228301

PACS numbers: 82.70.Dd, 64.75.Yz

Much of novel physics revolves around manmade structures of reduced dimensionality such as carbon nanotubes [1] or graphene [2]. Equally interesting yet far less explored are the mesoscopic analogs of these 1D and 2D materials built from colloidal particles [3] by relying on self-assembly as the strategy of choice at the micrometer length scale [4]. To induce the formation of a desired target structure and to ensure its stability, self-assembly requires close control of interparticle interaction. This remains among the most important challenges in colloid science [5–7]. The heart of the problem is the strength of the van der Waals attraction among the particles. Once they come into contact, they form irregular clusters which cannot be redispersed by thermal agitation and whose morphology is determined by the kinetics of aggregation [8–11]. To prevent this scenario and to equilibrate ordered structures, the interparticle interaction is usually engineered by polymer or charge stabilization [12] and index matching [13] but these protocols typically drive the common spherical colloids into bulk rather than 1D or 2D aggregates [14].

Alternatively, colloidal self-assembly can be directed by external fields. A static field induces either chainlike clusters characteristic of electro- and magneto-rheological fluids or bulk crystals [15–17]. In an alternating field, on the other hand, colloids may assemble into sheets: A rotating planar field generates an inverted  $r^{-3}$  dipolar pair interaction with in-plane attraction and repulsion along the rotation axis, which forces the particles into flat sheets parallel to the field plane [18]. In the so-called balanced triaxial field, the polarization forces between colloids are far more subtle—the pair interaction is isotropic—[19,20] and they were theoretically predicted to produce stable membranes of all orientations [19]. In this Letter, we substantiate this prediction by experimental observations of one-particle-thick membranes formed by micrometer-size spheres in a magic-angle precessing field [21]. We analyze in detail the aggregation process in this field configuration and we

demonstrate that it is governed by the many-body interactions.

In our experiment, we studied the behavior of a suspension of 1.05  $\mu\text{m}$ -diameter superparamagnetic spheres (Dynabeads, MyOne Carboxy; dissolved in Dynabeads solution to prevent sticking and sandwiched between two cover slips 100  $\mu\text{m}$  apart) subjected to a combined static and rotating magnetic field produced by three orthogonal pairs of Helmholtz coils [Fig. 1(a)]. Typical flux was 2.5 mT and the precession frequency was 400 Hz; to suppress net rotation of particles, the field was rotated back and forth by 360°. To facilitate manipulation of

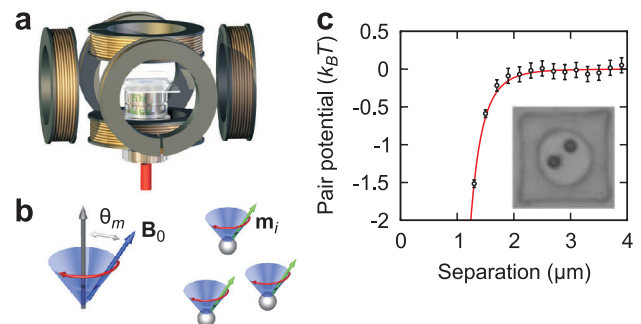


FIG. 1 (color online). Colloids in precessing magnetic field: The vertical coils generate the static component and the two horizontal pairs produce the rotating field (a). The cell is located in the center and the laser tweezers' beam enters the setup from below. The field cone opening angle  $\theta_m$  depends on the relative magnitude of the static and the rotating component (b). To lowest order, the induced magnetic moments of the colloids  $\mathbf{m}_i$  follow the external field. The pair potential  $U_2(r)$  (c) was measured by analyzing the motion of two colloids in a microfluidic chamber 5.5  $\mu\text{m}$  in diameter and 1.1  $\mu\text{m}$  in height (inset). By comparing their spatial distribution in zero field to that with the field on [26], we verified that  $U_2(r) \propto r^{-6}$  (red curve) and determined the susceptibility of the particles  $\chi = 0.89$ , which is consistent with earlier reports [27].

colloids and their aggregates, the setup is equipped with laser tweezers (Zeiss Axiovert 200M inverted microscope; Coherent Compass 2500MN continuous-wave Nd:YAG laser; AA Opto-Electronic DTSXY-250-1064-002 acousto-optic deflectors; Aresis Tweez beam-steering controller).

The field-induced interaction of two colloids separated by  $r$  is usually controlled by the  $r^{-3}$  term whose nature depends on the opening angle  $\theta_m$  of the field cone. For small  $\theta_m$ , the colloids behave like ordinary dipolar fluids [16] whereas opening angles close to  $90^\circ$  generate an effective in-plane attraction [18,22]. But at the magic opening angle  $\theta_m = \arctan(1/\sqrt{3}) \approx 54.7^\circ$  the time-averaged  $r^{-3}$  interaction term vanishes irrespective of the relative position of colloids in three dimensions. In this case, the leading-order nonzero term of the pair interaction is isotropic, attractive, and proportional to  $r^{-6}$  just like the van der Waals interaction between molecules [19,20]:  $U_2 = -3\chi^3 V^3 B_0^2 / 8 / \pi^2 \mu_0 r^6$  [Fig. 1(c)]. Here  $\chi$  and  $V$  are the susceptibility and the volume of the colloids, respectively, and  $B_0$  is the magnetic flux.

In the magic-angle field, we observed that a dilute suspension of colloids readily formed randomly oriented dimers, which shows that the pair interaction is isotropic. We quantified the interaction by analyzing the spatial distribution of two colloids in a microfluidic chamber and verified the  $r^{-6}$  power law. In the semidilute regime, formation of larger clusters followed a pathway epitomized by Fig. 2. Initially, the clusters were linear and grew by terminal addition of particles; at the magic angle the spatial orientation of chains was entirely random. After chains reached the length of about 8 particles, their middle sections became decorated by laterally attached colloids. These Y junctions served as branching points and in the next stage the branched chains interconnected into a network with a well-defined length scale. Finally, the network underwent gradual coarsening which included contraction of loops and folding of side chains and produced sizable membranelike patches of all orientations. In a semidilute suspension, the last stage of aggregation was rather slow but in a dense suspension large membranes of close-packed colloids appeared almost instantaneously.

The membrane formation pathway is unlike any classical aggregation scenario including diffusion- or reaction-limited aggregation, spinodal decomposition, and nucleation, and it is driven entirely by the magnetic forces—after the field is turned off, the membranes are immediately disintegrated. To explain the observed aggregation process, we theoretically studied the interactions among the colloids which are inherently nonpairwise additive. We computed self-consistently the induced magnetic moment  $\mathbf{m}_i(t)$  of each colloid in the local field  $\mathbf{B}_{\text{local}}(\mathbf{r}_i, t) = \mathbf{B}_0(t) + \sum_j \mathbf{B}_j(\mathbf{r}_j - \mathbf{r}_i, t)$  which consists of the external field and the fields produced by the induced dipoles of all other colloids [19]. The  $\mathbf{m}_i$ 's were then used to evaluate the time-averaged magnetic energy  $E = -(1/2) \times \langle \sum_i \mathbf{m}_i(t) \cdot \mathbf{B}_{\text{local}}(\mathbf{r}_i, t) \rangle$  (the angle brackets denote averaging over 1 field cycle) as well as the many-body potentials of a set of representative aggregate morphologies. In our experiment, the binding energies of aggregates far exceed the thermal energy  $k_B T$  which justifies the zero-temperature description used here.

We first computed the potential experienced by a test particle close to a dimer, which is attractive along the dimer axis and has a barrier in the lateral direction. The lateral repulsion is entirely due to the three-body interactions: If the potential were a sum of the three pair interactions, it would have been attractive in all directions. Although qualitatively analogous, our three-body term is stronger relative to the pair interaction than the Axilrod-Teller three-body dispersion interaction in van der Waals systems [23]. In an external field of 2.5 mT used in our experiments, the calculated height of the lateral barrier is about  $0.65k_B T$  whereas the depth of the attractive well along the dimer axis is about  $-22k_B T$ . Consequently, a test particle located anywhere close to the dimer is dragged strongly towards the nearer end.

The lateral barrier of a short chain is similar to that of a dimer [Fig. 3(a)]. But in chains of more than about 8 colloids the central section of the barrier is saddle shaped [Fig. 3(b)]. The midchain barrier decreases with the chain length from about  $1.65k_B T$  in a tetramer to below  $1k_B T$  in an eight-colloid chain and then to virtually zero in chains

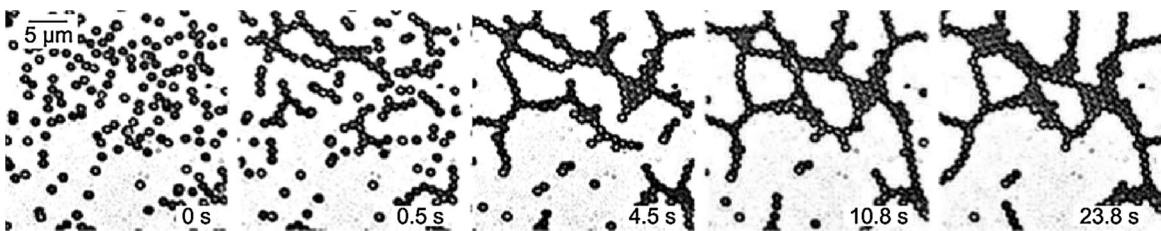


FIG. 2. Snapshots of the evolution of a dilute suspension (0.15 particles per  $\mu\text{m}^3$ ) after the field has been switched on. The virtually instantaneous appearance of short chains (0.5 s) is followed by their growth, branching, and formation of a loose network (4.5 s). Most remaining unconnected clusters are rapidly captured and the network is subsequently coarsened such that the membrane patches grow at the expense of the chainlike sections (10.8 s and 23.8 s). The distance between adjacent vertices of the network does not exceed the branching length of about 8 colloids. Shown here is a small part of the field-of-view where the majority of the colloids confined to a  $100 \mu\text{m}$ -thick cell are in the focal plane.

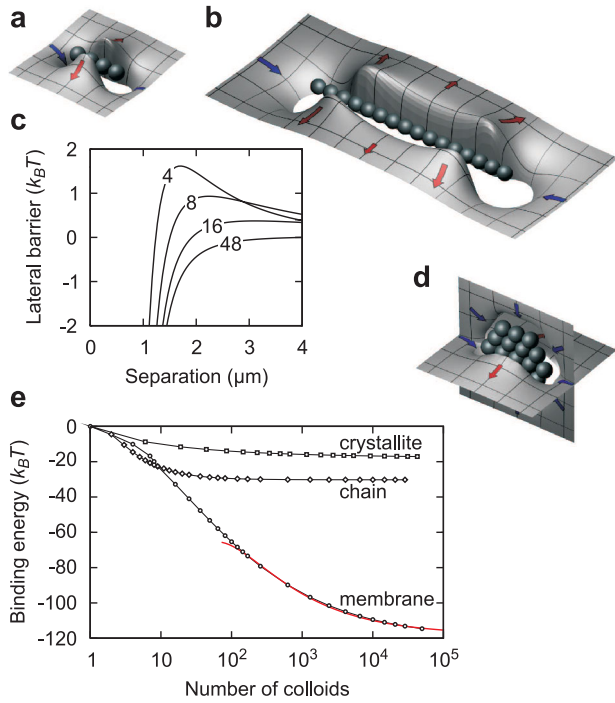


FIG. 3 (color online). Computed potential of a test colloid near a straight 4-colloid chain in a plane that includes chain axis (a): The colloid is drawn to the ends so as to make the chain grow lengthwise, whereas a sideways approach is prohibited by the potential barrier whose magnitude is largest in the normal plane through chain center. With increasing chain length, the lateral barrier along the midline decreases; panel (b) shows the potential of a 16-colloid chain and panel (c) depicts the profile of the midline lateral barrier of 4-, 8-, 16-, and 48-colloid chain. Potential of a membrane patch (d) is attractive along the perimeter and repulsive normal to the patch. Energy per particle in chain, membrane, and crystallite in a field of 2.5 mT vs cluster size (e): The red (light gray) curve is the fit described in the text and the thin black lines are the guide to the eye. The data correspond to rhombic close-packed membranes and bipyramidal close-packed crystallites; except in small clusters, the more isotropic shapes produce very similar results.

of more than about 30 colloids [Fig. 3(c)]. In chains of more than 8 colloids, the probability for a particle to cross the lateral barrier near chain center and laterally attach to the chain becomes sizable.

These arguments explain the absence of isolated long chains. The exclusive mode of growth of short chains is terminal attachment but after they reach the length of about 8 colloids, lateral attachment becomes dominant. At this point, chains start to branch and form a network with a characteristic length of about 8 colloids. The branching length  $L^* \approx 8$  (i.e., the maximal number of particles in an unbranched chain segment) is a clear manifestation of the many-body interactions. In turn, branching alters the potential landscape around a chain. Our theoretical analysis has shown that the local in-plane potential around a  $Y$  junction is attractive, which promotes the formation of

small patches (Fig. 2). Their subsequent coarsening leading to membranes can be explained by evaluating the potential of a test particle close to a planar patch, which is attractive at the perimeter and repulsive in the normal direction [Fig. 3(d)].

Another way of looking at the stability of membranes is to compare the binding energies of colloids in different close-packed configurations [Fig. 3(e)]. In infinite clusters, the binding energy per particle in a chain, membrane, and crystallite is about  $-31k_B T$ ,  $-119k_B T$ , and  $-17k_B T$ , respectively. Clusters of up to 9 particles prefer chains to membranes, the location of the chain-to-membrane crossover being consistent with the branching length  $L^*$ . A complementary interpretation of  $L^*$  comes from a phenomenological model of membrane patches where all particles within the perimeter strip of width  $z$  are assigned an excess surface energy  $\gamma$  relative to those in an infinite membrane  $E_\infty$  so that the energy per particle in a square membrane of  $N$  colloids reads  $E(N) = E_\infty + 4z\gamma N^{-1/2}(1 - zN^{-1/2})$ . This model reproduces the energy of patches with more than about 100 colloids [red (light gray) line in Fig. 3(e)], the best-fit model parameters being  $E_\infty = -119k_B T$ ,  $z^* = 4$ , and  $\gamma^* = 52k_B T$ . The same type of model can be used for chains; in this case,  $z^*$  represents the length of the end caps where the binding energy per colloid is larger than in an infinite chain. Chains of less than  $2z^* = 8$  colloids consist solely of the two caps whereas the longer chains also include a core, and the transition from the cap-cap to cap-core-cap regime coincides with the branching length of  $L^* = 8$ .

The behavior of semidilute samples provides a clear insight into the kinetics of aggregation (Fig. 2), but the final structure is arrested and gel-like. Fabrication of large membranes was easiest in dense suspensions: We first let the colloids sediment to increase the local density at the bottom of the cell and then we turned on the field. Within seconds, large close-packed membranes formed parallel to the bottom slide, which were then studied by analyzing their response to external perturbation.

Figure 4(a) shows four horizontal slices through a curved membrane folded upwards by decreasing the opening angle of the field cone by about  $1^\circ$ , which pulled a part of the membrane in the vertical orientation without affecting its integrity [24]. This demonstrates that the membranes are flexible and can be tailored into hollow shapes such as tubes. Another way of membrane manipulation that we explored was to introduce a few large  $9 \mu\text{m}$  silica colloids and use them as anchors. In the side views of a section of a membrane spanned by such anchors seen in Fig. 4(c), the anchor located in the center was held by laser tweezers and pushed against the membrane so as to bend it up to the point when the membrane was perforated. The time-sequence snapshots [Fig. 4(c)] demonstrate that the membrane was spontaneously reconstituted immediately after the central anchor had passed through it. The self-

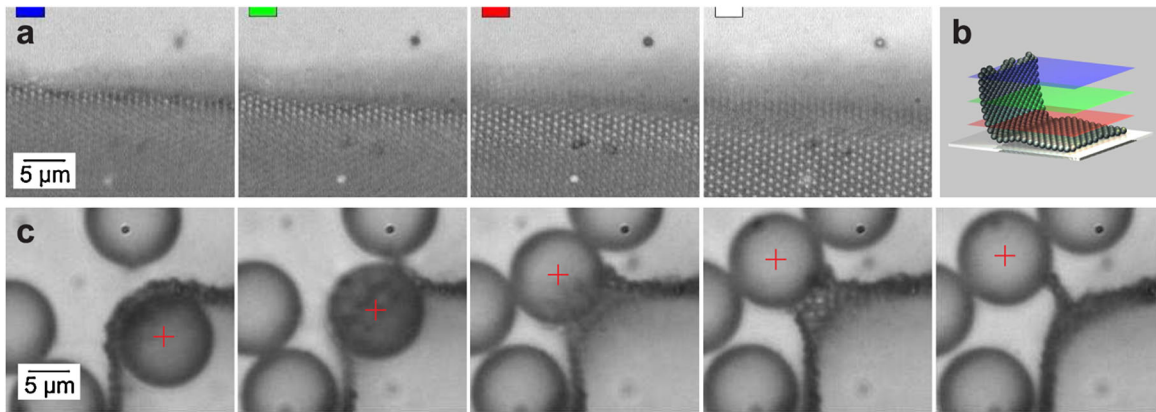


FIG. 4 (color online).  $z$  scan through a colloidal membrane partly lying on the bottom slide (a) and schematic interpretative image of the membrane (b). The four micrographs obtained by moving the focal plane from top to bottom disclose the vertical, the curved cylindrical, and the flat horizontal part of the membrane. Time-sequence micrographs of the passage of a  $9\ \mu\text{m}$  colloid through a membrane (c). As the large colloid held by laser tweezers and marked by a red cross is pushed against it, the membrane bends until it breaks so that the colloid can pass through it; after that the membrane is self-healed spontaneously.

healing behavior can be understood easily: A single hole in the membrane increases the energy of about  $L^{*2} = 64$  colloids around it and the theoretical energy cost in a field of 2.5 mT amounts to about  $300k_B T$ .

Our experiment reveals a nonspecific aggregation pathway leading to robust one-particle-thick membranes, which could conceivably be folded into closed morphologies by adding small or anisometric particles that would act as defects. The many-body polarization interactions essential for the phenomena described above are very similar to the van der Waals force [12] between atoms and molecules except for the coherence of the dipoles induced by the driving field. It is tempting to speculate that some degree of coherence of fluctuating dipoles may be stimulated at the molecular level, e.g., by optical field or spatial confinement, thereby opening a route to self-assembled planar and shell-like nanostructures [25].

We thank H. H. von Grünberg, R. D. Kamien, J. Kotar, M. E. Leunissen, C. N. Likos, M. A. Miller, R. Podgornik, and A. Šiber for stimulating discussions. This work was supported by Slovenian Research Agency through Grants No. J1-6502 and No. P1-0055, by European Research Council through the Advanced Research Grant No. RG52356, and by Royal Society Wolfson Grant No. RG50421.

- 
- [1] R.H. Baughman, A.A. Zakhidov, and W.A. de Heer, *Science* **297**, 787 (2002).
  - [2] A.K. Geim and K.S. Novoselov, *Nature Mater.* **6**, 183 (2007).
  - [3] P. Akcora *et al.*, *Nature Mater.* **8**, 354 (2009).
  - [4] G.M. Whitesides and M. Boncheva, *Proc. Natl. Acad. Sci. U.S.A.* **99**, 4769 (2002).

- [5] V.J. Anderson and H.N.W. Lekkerkerker, *Nature (London)* **416**, 811 (2002).
- [6] S. Glotzer, M.J. Solomon, and N.A. Kotov, *AIChE J.* **50**, 2978 (2004).
- [7] E. Zaccarelli, *J. Phys. Condens. Matter* **19**, 323101 (2007).
- [8] T.A. Witten and L.M. Sander, *Phys. Rev. Lett.* **47**, 1400 (1981).
- [9] D.A. Weitz and M. Oliveria, *Phys. Rev. Lett.* **52**, 1433 (1984).
- [10] D.W. Schaefer *et al.*, *Phys. Rev. Lett.* **52**, 2371 (1984).
- [11] M.Y. Lin *et al.*, *Nature (London)* **339**, 360 (1989).
- [12] J.N. Israelachvili, *Intermolecular and Surface Forces* (Academic Press, London, 1991).
- [13] R.P.A. Dullens *et al.*, *Langmuir* **19**, 5963 (2003).
- [14] Y.N. Xia *et al.*, *Adv. Mater.* **12**, 693 (2000).
- [15] A. Yethiraj and A. van Blaaderen, *Nature (London)* **421**, 513 (2003).
- [16] U. Dassanayake, S. Fraden, and A. van Blaaderen, *J. Chem. Phys.* **112**, 3851 (2000).
- [17] M.E. Leunissen, H.R. Vutukuri, and A. van Blaaderen, *Adv. Mater.* **21**, 3116 (2009).
- [18] N. Elsner *et al.*, *J. Chem. Phys.* **130**, 154901 (2009).
- [19] J.E. Martin, R.A. Anderson, and R.L. Williamson, *J. Chem. Phys.* **118**, 1557 (2003).
- [20] J.E. Martin *et al.*, *Phys. Rev. E* **69**, 021508 (2004).
- [21] P. Tierno, R. Muruganathan, and T.M. Fischer, *Phys. Rev. Lett.* **98**, 028301 (2007).
- [22] B.A. Grzybowski, H.A. Stone, and G.M. Whitesides, *Nature (London)* **405**, 1033 (2000).
- [23] B.M. Axilrod and E. Teller, *J. Chem. Phys.* **11**, 299 (1943).
- [24] Conversely, a small increase of the field cone opening angle induces a horizontal membrane orientation.
- [25] K. Van Workum and J.F. Douglas, *Phys. Rev. E* **73**, 031502 (2006).
- [26] M. Brunner *et al.*, *Phys. Rev. Lett.* **92**, 078301 (2004).
- [27] G. Fønnum *et al.*, *J. Magn. Magn. Mater.* **293**, 41 (2005).